Journal of Constructional Steel Research 219 (2024) 108793

Contents lists available at ScienceDirect

Journal of Constructional Steel Research

journal homepage: www.elsevier.com/locate/jcsr

Vibration performance of cold-formed steel and plywood composite floors – Experimental studies

Suleiman A. Al-Hunaity, Harry Far *

School of Civil and Environmental Engineering, Faculty of Engineering and Information Technology, University of Technology Sydney (UTS), Sydney, Australia

ARTICLE INFO

Keywords:
Cold-formed steel
Composite floors
Vibration performance
Dynamic properties
Steel

ABSTRACT

Cold-formed steel and timber composite floors are lightweight structures with relatively high stiffness, allowing for longer spans. Consequently, they demonstrate inherent characteristics of reduced fundamental natural frequency and damping compared to conventional counterparts, rendering them prone to vibrations induced by human activities such as walking and dancing. This study delves into the dynamic performance of such lightweight floors, comprising cold-formed steel joists and plywood panels. Employing modal testing alongside deflection assessments, twelve full-scale composite floors were subjected to analysis to elucidate their dynamic attributes, including natural frequencies, mode shapes, and flexural stiffness. The findings unveiled that composite floors constructed with cold-formed steel and plywood, featuring a span length of 4.50 m, manifested fundamental natural frequencies exceeding 8 Hz. Furthermore, assessments of flexural stiffness derived from vibration and deflection tests suggested a robust composite action, with minimal slip observed at the interface between plywood panels and cold-formed steel joists.

1. Introduction

The competitive trends in the construction industry have redirected the research compass towards practical, sustainable, and more importantly, energy-efficient structural solutions to compete with conventional structural systems, such as reinforced concrete floors [1,2]. Additionally, long span floors with minimum intermediate supports became increasingly of interest in recent years [3]. Recently, composite floors comprising of cold-formed joists and timber flooring panels earned strategic importance in the construction industry in Europe, North America, Australia, and New Zealand, especially the residential and high-rise building sectors [4,5], owing to their lightness, design flexibility, rapid onsite assembly, dimensional stability, and a high strength-to-mass ratio [6,7].

Among different types of composite floors, cold-formed steel and timber composite floors combine a supporting cold-formed steel joists with engineered mass timber panels, such as plywood panels, Cross Laminated Timber (CLT), or Glue Laminated (GL) lumber, to create a composite flooring system with higher span-to-depth ratio. Cold-formed steel joists, which mainly resist tensile stresses, enhances the bearing capacity and ductility and reduces the self-weight of the floors [8,9], whereas, timber floor panels contributes to the lightness of the floors and offers numerous advantages, such as structural in-plane stability, low embodied energy, low carbon footprint, and the ability to recycle and replace the decayed elements [7,10–12]. Moreover, the construction of composite floors comprised of engineered timber panels and cold-formed steel joists can be modularised [7], i.e. 70–95% of onsite assembly activities are replaced by off-site construction at a designated facility [3]. Modular Building Systems (MBS) are environmentally friendly and offers various advantages such as higher quality control, cost efficiency, and less construction time compared to monolithic building systems [13,14].

The efficiency of composite floors is primarily attributed to the achieved degree of composite action which is governed by the behaviour of the shear connection between the cold-formed steel joists and timber slabs [3,15–17]. Shear connections in composite construction are essentially designed to endure the horizontal shear forces that develop between the joist flange and top slab and endure the uplift loads between them [18]. Different types of connections were proposed in the literature including mechanical fasteners (e.g. self-drilling screws and bolts) [19,20], adhesives [7,21], and steel mesh plates [20,22].

Cold-formed steel and timber composite flooring systems are lightweight and allow for longer spans, thus, they are likely to experience uncomfortable floor vibrations due to human activities such as walking

* Corresponding author.
E-mail address: Harry.Far@uts.edu.au (H. Far).

https://doi.org/10.1016/j.jcsr.2024.108793
Received 8 January 2024; Received in revised form 17 April 2024; Accepted 21 May 2024
Available online 3 June 2024

and dancing [23,24]. The deflection and vibration serviceability criteria often governs the design of cold-formed steel and timber composite floors [25], whilst the ultimate bearing capacity of the floors is generally several times higher than the design load level of the structure. When timber panels are connected to cold-formed steel joists using high-performance dowels, the static flexural stiffness is considerably increased [26–28]. However, the addition of timber panels does not guarantee a satisfactory vibration performance of the floors. The fundamental natural frequency may deteriorate if the increase in stiffness is not enough to offset the increase in mass [25]. Therefore, the dynamic behaviour of the composite floors can be a decisive criterion in the design of modern open floor layouts with longer span and lower damping compared to traditional floors with partitions and heavy furniture [29].

Numerous studies have been carried out to measure and evaluate the vibration behaviour of composite floors made of cold-formed steel and timber. Zhang et al., [25] conducted a series of modal testing on concrete-timber composite floors to evaluate their dynamic response. According to the test results, the fundamental natural frequencies of the tested floors, with 6 m span, were generally found to be above 8 Hz and that adding a layer of concrete to the timber panels enhanced the floor's fundamental natural frequency and its damping. Cao et al., [30] performed field tests to examine the vibration behaviour of steel composite floors. The research concluded that the damping ration of the studied floors can be minimised by improving the human-structure interaction. Xu et al., [5] derived analytical formulas to analyse the dynamic behaviour of composite floors made of cold-formed steel and timber under three types of loadings. Their research studied how different factors, such as boundary conditions and mass ratios, affect the dynamic response. Their findings suggest that altering the boundary conditions may not decrease the floor vibration response and that the effect of small mass ratios on the floor dynamic behaviour is negligible. Overall, the existing studies only focused on certain structural geometries, and their established standards were based on the local practices. Therefore, these results may not be suitable for different structures and countries without careful consideration [31].

Design guidelines of ISO 10137 [29,32] and AISC are frequently applied to evaluate concrete and steel composite flooring systems having Eigen-natural frequency lower than 8.0 Hz [25]. The applicability of such guidelines to cold-formed steel and timber composite floors is doubtful, which is attributed to lack of the available test data. Also, the effect of timber panel on enhancing the vibration behaviour of the bare cold-formed steel joists is generally disputed. While the addition of timber panels is intended to improve the vibration behaviour of the joists, it may also decrease the floor's fundamental natural frequency due to the increase in mass. Moreover, previous research on cold-formed steel and timber composite floors focused on enhancing the composite action efficacy of the floors subjected to static loads through testing various shear connections arrangements. Conversely, the vibration performance of the cold-formed steel and timber composite floors, which can control the floor span and its thickness at the design stage, have not been well examined. Therefore, the need arises to evaluate the dynamic behaviour of such lightweight floors at the design stage to avoid the occurrence of vibration problems in future. In response to this imperative, the present study strides towards these objectives by conducting experimental analyses on the dynamic attributes of the flooring system, encompassing natural frequencies, mode shapes, and flexural stiffness. It's imperative to highlight that the research team spearheading this project is actively working towards addressing the identified needs above, with this manuscript forming a crucial component of our collective efforts in this regard.

It is emphasised that the assessment of vibrations for the tested composite floors has been previously published [33] and should be considered in conjunction with the current study. Al-Hunaity & Far (2024) [33] extensively explores the structural evaluation of floors, conducting thorough parametric studies that broaden the scope of this study. In the preceding study [33], a finite element model was developed, updated, and validated against experimental results presented in this study to scrutinise the influence of design parameters on vibration properties. Notably, numerical analyses revealed that as added mass exceeded stiffness enhancement, the fundamental natural frequency decreased, whereas thicker and deeper joist sections increased fundamental natural frequency by enhancing stiffness. Expanding upon these numerical insights, the current study prioritises experimental aspects, scrutinising the dynamic attributes of the flooring system, including natural frequencies, mode shapes, and flexural stiffness.

The primary objective of the present study is to investigate the dynamic performance of cold-formed steel and plywood composite floors and assess their static and bending flexural stiffness. Modal testing was conducted on twelve full scale composite floors considering simply supported conditions. Using modal analysis techniques, the natural frequencies, damping ratios, and mode shapes (known as the modal properties) of the floors were extracted. Additionally, static deflection tests under concentrated 1 kN load was carried out. Also, the flexural stiffness of the tested composite floors calculated from the modal tests were compared to flexural stiffness calculated from deflection tests and four-point bending tests. Moreover, the effect of utilising different types of fasteners and spaced at various intervals was investigated.

2. Experimental program

The extensive experimental program adopted in this research project is illustrated in Fig. 1. Material tests were first conducted to evaluate the mechanical properties of the plywood panels and cold-formed steel joists. Then, push out tests were conducted to explore the failure patterns and the mechanical properties of the composite cold-formed steel and plywood connections. Finally, dynamic behaviour of the cold-formed steel and plywood composite floors was explored. Material and push out test results were reported and discussed in separate papers [15,34]. Accordingly, this study discusses in detail the findings of the dynamic tests conducted on the composite floors.

2.1. Materials

Locally sourced plywood panels along with standard Australian cold formed steel C-sections were used to fabricate the composite floors. Several tests, including tensile, compressive and bending tests, were conducted on the plywood panels and cold-formed steel joists and their corresponding full results, such as dimensions and mechanical properties, were discussed and reported in a separate paper [15,34]. Tables 1 and 2 summarise the average mechanical properties of the plywood panels and cold-formed steel joists, respectively.

Three different types of shear dowels were employed in the fabrication of the composite floors including Self-drilling Screws (SDS) (diameter: 6 mm, length: 47 mm, material: low carbon steel), coach screws (CS) (diameter: 12 mm, length: 45 mm, material: low carbon steel), and bolts diameter: 8 mm and 12 mm, length: 75 mm and 80 mm, grade: 4.6). All fasteners were procured from the local market and were manufactured according to relevant Australian Standards [35,36].

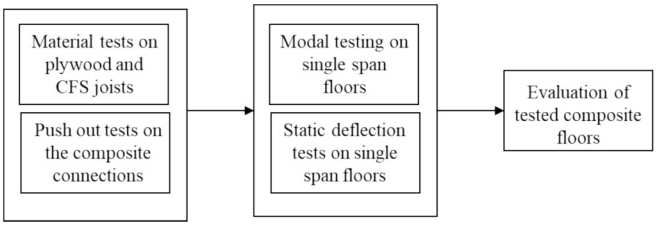

Fig. 1. Experimental program on cold-formed steel and plywood composite floors.

Table 1
Mechanical properties of cold-formed steel joists.

Section depth (mm)	Thickness (mm)	Yield strength (MPa)	Ultimate strength (MPa)	Elastic modulus (MPa)	Elongation at fracture (%)
254	2.4	500	560	205,000	13

2.2. Geometry and details of tested specimens

A total of twelve composite floor samples were fabricated and tested in this study. The investigated composite floors are comprised of two cold-formed steel joists and connected to two plywood panels to achieve the full length of the floor. The centre-to-centre spacing between the joists is 600 mm. The total length of the samples was 4.70 m; however, the corresponding supported span is 4.50 m. In general, all specimens were identical in terms of cross-sectional geometry but varied in the type and spacing of fasteners, presence of structural epoxy resin at the interface between the joists and plywood, and web holes cut through the joist's web. Table 3 provides the basic parameters for each specimen, whereas Fig. 2 shows the details of the tested composite floors.

Specimen 1 was designed as the reference sample. Specimen 1 utilises 6 mm SDS connectors spaced at 400 mm. Similarly, 6 mm SDS fasteners spaced at 200 mm are used to fabricate specimen 2. Specimens 3 and 4 used M12 CS with 400 mm spacing; however, in specimen 3, structural epoxy resin was applied at the interface between the joist top flange and plywood panels. Specimen 5 employed M12 CS spaced at 200 mm. M12 nuts and bolts shear connectors with 400 mm spacing were utilised to construct specimen 6. Specimens 7 and 8 are identical (M12 bolts spaced at 800 mm) except structural epoxy resin is applied between the joists and plywood in specimen 7. Specimens 9 and 10 varied only in fasteners spacing, that is, 200 mm and 400 mm, respectively, whereas the fastener type (M8 bolts) was maintained identical. Finally, joists with web openings for utilities are common in practice; therefore, Specimens 11 and 12 were fabricated from joists having web openings to examine the influence of web openings on the vibration behaviour of the cold-formed steel and plywood composite floors. The openings had a 100 mm diameter and were spaced at 300 mm on centre as shown in Fig. 3. In the fabrication of the samples utilising M8 bolts, M12 bolts, and M12 CS, pilot holes were pre-drilled into the cold-formed steel joists and plywood panels. For bolted and coach screw connections, the diameter of the pre-drilled holes in the plywood panels was 1–2 mm larger than the bolt's diameter and 2 mm smaller than the coach screw diameter. Pre-drilled holes in the cold-formed steel joists had a diameter of 0.5 mm greater than the diameter of the connectors (screws and bolts). Considerations were taken to ensure the holes in plywood and joists were perfectly coincident. Pre-drilling of plywood was unnecessary for specimens with SDS dowels as screws were directly drilled into the panels.

2.3. Methodology

Impact hammer with a medium tip (Fig. 4a) was used to excite the cold-formed steel and plywood composite floors at five different locations. The first, fourth, and fifth impact locations were hammered to excite the flexural modes, whereas the second and third location were primarily hit to excite the torsional mode shapes. Twenty-four piezoelectric accelerometers (nominal sensitivity 1.02 mV/g, frequency range of 0.5–10,000 Hz), shown in Fig. 4b, were mounted on each floor specimen to measure the vibration response and capture the relevant mode shapes accurately up to 200 Hz. All the accelerometers were mounted on top of the plywood panels using a 25 × 25 × 3 mm steel chips glued to the plywood panels, then rare earth neodymium magnets were used to firmly fix the accelerometer to the steel chip. Fig. 4c captures the input hammer excitation and its corresponding output acceleration during testing, whereas Fig. 4d depicts a composite floor specimen ready for testing.

It is highlighted that each hammer location was hit five times, i.e., each floor was hit twenty-five times to precisely measure the first seven natural frequencies and mode shapes. For each hammer location, the acquired frequency response functions (FRFs) were averaged to obtain a smooth FRF. The raw data was acquired using multichannel modular analyser (PXI, National Instruments) and a PC based data acquisition system (LabVIEW) (Fig. 4c). Fig. 4d shows a typical modal testing setup, whilst Fig. 5 depicts the spatial location of the accelerometers and hammering locations. After the modal testing of each floor concluded, static deflection tests were conducted to measure the vertical deflection of the tested floor under 1 kN concentrated load placed at mid-span of the composite floor sample. Two linear variable differential transformers (LVDTs), with a stroke of ±50 mm, were employed to measure the vertical deflection of the tested floor. The recorded displacement was then taken as the average of the LVDTs readings. Location of the LVDTs is shown in Fig. 6.

All composite floors were tested under a simply supported boundary conditions. Composite floor samples were resting on spherical supports that are mounted on heavy concrete blocks (Fig. 7). The spherical supports were able to accommodate the geometric imperfections of the cold-formed steel flange and maintain a full contact between the supports and the tested floors. Further, Teflon pads were placed between the cold-formed steel flange and the spherical supports, as shown in Fig. 7, to minimise friction and avoid bouncing at supports.

Dynamic properties of the cold-formed steel and plywood composite floors, including natural frequencies, mode shapes and damping, were extracted from the acquired Frequency Response Functions (FRFs), which are obtained from vibration testing. FRFs are a set of function which relate the exciting force to the corresponding vibration responses at various positions along the specimen with sufficient spatial and frequency resolution [37]. Time histories of the applied forces and their corresponding responses are transferred into FRFs by using spectral analysis (Eq. (1)). Subsequently, a curve fitting technique is applied to estimate FRFs with adequate accuracy. Modal properties, such as natural frequencies, damping ratios, and mode shapes, are then calculated from the averaged FRFs [38].

Table 3
Key parameters of the tested composite floors.

Specimen	Fastener	Spacing (mm)	Structural Epoxy	Web Holes
1	SDS 6 mm	400	–	–
2		200	–	–
3	M12 CS	400	True	–
4		400	–	–
5		200	–	–
6		400	–	–
7	M12 Bolts	800	True	–
8		800	–	–
9	M8 Bolts	200	–	–
10		400	–	–
11	M12 Bolts	800	–	True
12	M12 CS	200	–	True

Table 2
Mechanical properties of plywood panels.

Density (kg/m^3)	Bending strength (MPa)	Parallel-to-grain tensile strength (MPa)	Parallel-to-grain compression strength (MPa)	Elastic modulus (MPa)	Shear modulus (MPa)	Poisson's ratio
500	40	15	30	10,200	41.50	0.3

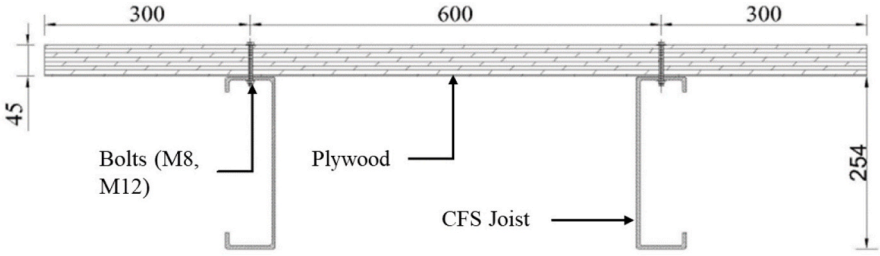

(a) Cross section of composite floor specimens utilising bolts as shear connectors

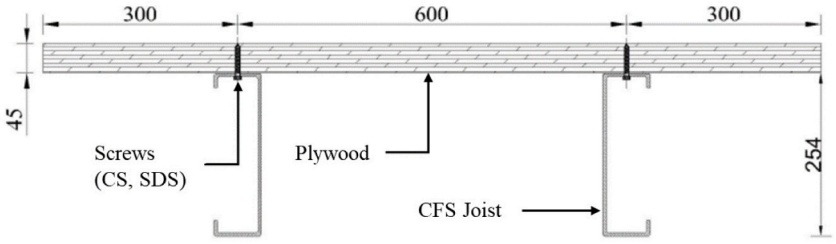

(b) Cross section of composite floor specimens utilising screws as shear connectors

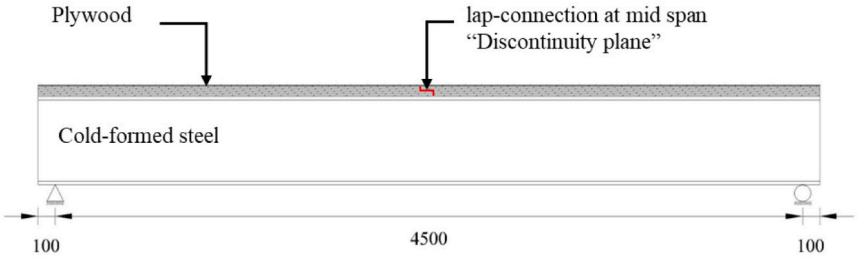

(c) Composite floor specimens – Side view

Fig. 2. Typical cross section and side views of composite floor specimens (all dimensions are in mm).

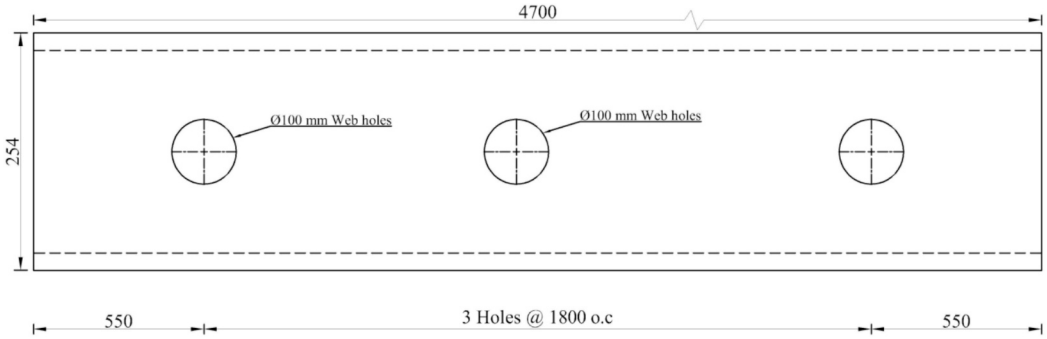

Fig. 3. Details of web openings (location and size) drilled through the joist's web (all dimensions are in mm).

$$H(\omega) = \frac{G(\omega)_{yy}}{G(\omega)_{xx}} \tag{1}$$

where, $H(\omega)$ is the frequency response function, $G(\omega)_{yy}$ is the Power Spectral Density of the response, and $G(\omega)_{xx}$ is the Power Spectral Density of the excitation force.

The quality of the obtained data can be evaluated by the coherence function, which indicates how much input data is involved in the output data [38]. The value of the coherence function ranges between 0 and 1. A value of zero indicates a weak correlation between input and output data, and a value of 1 represents the ideal case. The coherence function is defined in Eq. (2).

$$\gamma(\omega)_{xy} = \frac{\left|G(\omega)_{xy}\right|}{G(\omega)_{xx}{}^{*}G(\omega)_{yy}} \tag{2}$$

where, $\gamma(\omega)xy$ is the coherence function, and $G(\omega)xy$ is the Cross Power Spectral Density of the response between input and output data.

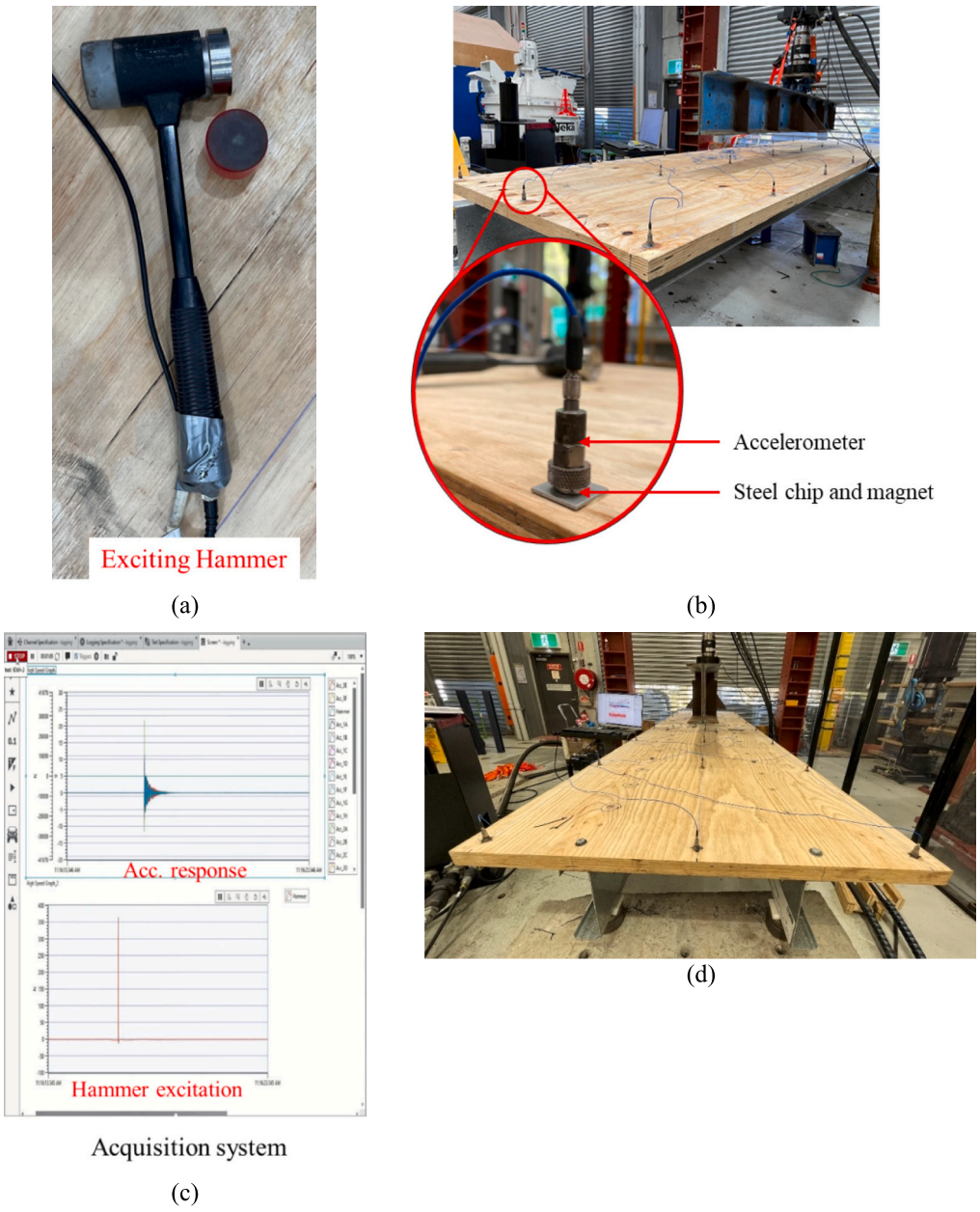

Fig. 4. Typical modal testing arrangement; (a) Medium tip excitation hammer, (b) detailing of accelerometers attachment method, (c) Acquisition system, and (d) Sample floor ready for testing.

3. Test results and discussions

3.1. Dynamic properties

Modal parameters including natural frequencies, damping ratios, and mode shapes, of the tested cold-formed steel and plywood composite floors were calculated from the experimental modal analysis carried out using Simcenter Testlab software [39]. The natural frequencies, mode shapes, and damping ratios were measured from the resonant frequencies in the calculated FRFs which were transformed from the measured time history acceleration responses utilising the Fast Fourier Transform (FFT). The first five flexural natural frequencies of the tested composite floors are listed in Table 4, where f_{11} is the first flexural frequency, f_{12} is the second flexural frequency, f_{13} is the third flexural frequency, whilst f_{21} and f_{22} are the first and second transverse flexural frequencies, respectively. Table 4 also lists the first and second torsional frequencies (denoted by f_{1t} and f_{2t}, respectively) of the tested composite floors. Accordingly, the corresponding mode shapes for the composite floors, depicted in Fig. 8, were calculated from the relative phase and amplitudes of the FRFs for natural frequencies at several points along the tested floor. A typical FRFs diagrams of specimen 3 are shown in Fig. 9. Fig. 9 also compares the floor responses when excited at H1 and H3 hammer locations. The depicted FRFs (frequency range 0–200 Hz)) were measured at the A10 accelerometer location due to an excitation at H1 and H3 hammer locations, respectively. As expected, flexural modes were dominant when point of symmetry was hit, i.e. location H1, whilst multiple torsional modes were excited when un-symmetric location (i.e. H3 location) was excited. It is noted that selecting location A10 was purely arbitrary and was chosen to serve as an illustrative example of the calculated Frequency Response Functions (FRFs).

3.2. Quality and validation of natural frequencies

To ensure the quality of the calculated FRFs, the coherence function

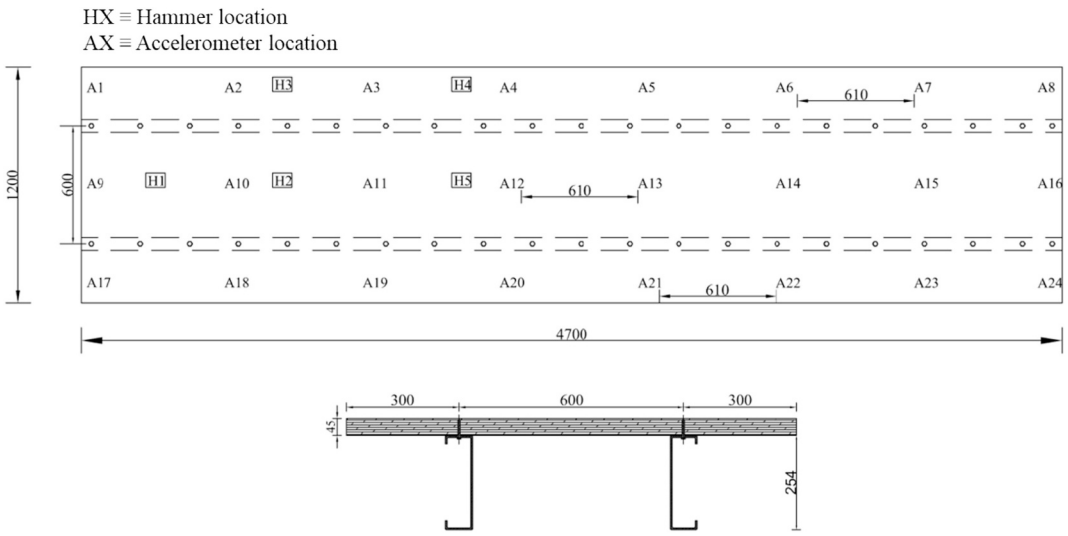

Fig. 5. Locations of accelerometers and locations of hammer impacts applied on the tested composite floor systems (all dimensions are in mm).

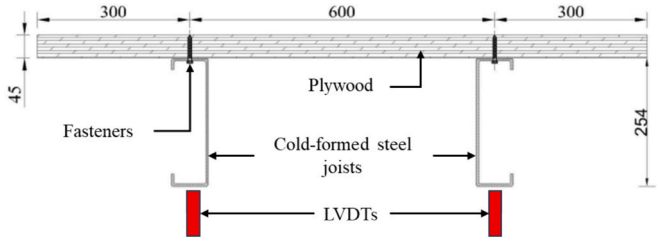

Fig. 6. Location of the two LVDTs used to measure the deflection at mid span due to 1 kN concentrated load.

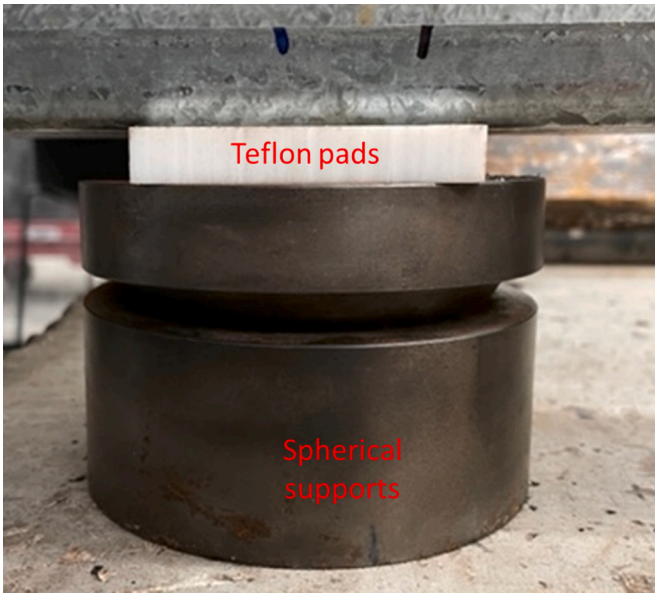

Fig. 7. Spherical boundary conditions utilised in modal testing to support the composite floor specimens.

was estimated at each hammer location. As discussed in Section 2, the coherence function specifies the degree to which the output data is related to the input data in an FRF, i.e. it measures the consistency of the FRF from a measurement to be replicated from the same measurement [40]. The coherence function takes values between 0 and 1, where 0 indicates the measurement is not repeatable, i.e., there is an error in the measurement, and 1 indicates the FRF phase and amplitude are highly repeatable. Coherence functions of specimens 2, 3, 6, and 9 are mapped in Fig. 10. It is obvious from Fig. 10 that the modal testing measurements yielded a highly repeatable FRFs. It is noted that the dips in the coherence diagram happen at the anti-resonance, i.e., when the amplitude of the FRF is low. This is normal in modal testing since the signals are weak at such points and their repeatability is inconsistent with noise floor of the instrumentation [39].

Two criteria were utilised to validate the calculated natural frequencies: namely, Modal assurance criterion (MAC) and modal synthesis. MAC is a validation tool that is used to determine the similarity of the calculated natural frequencies and their corresponding mode shapes. A value of 1 for the MAC indicates a high similarity between selected mode shapes, whereas a value of 0 MAC implies that the calculated mode shapes are unique in comparison with other calculated modes. MAC values of specimens 2 are illustrated in Fig. 11, which indicate that the selected mode shapes are unique and very different. Modal synthesis is a process where an FRF is generated from the modes found during modal curve fitting. This synthesised FRF can be compared to the actual measured FRF to see if there is a good match (Fig. 12). While the MAC can indicate if too many modes were selected, the modal synthesis can check if any modes were missed during the modal curve fitting process. An error percentage and correlation value are assigned to each synthesised FRF and its corresponding measured FRF. Accordingly, lower error percentage and higher correlation values indicate no mode shapes were missed during the curve fitting process. As part of the data post-processing procedure, synthesised Frequency Response Functions (FRFs) were calculated for all specimens to ensure comprehensive modal analysis coverage. It is notable that specimens 3 and 9 exhibited the highest error values. It is illustrated in the modal synthesis curves, shown in Fig. 12, that minimal error values of 7.33% and 6.99%was achieved for specimens 3 and 9, respectively. Accordingly, Table 5 tabulates the correlation values and their corresponding error compared to the actual measured FRFs for all specimens. (See Table 6.)

3.3. Discussion of vibration properties

3.3.1. Natural frequencies

Mass, span, flexural stiffness, and friction at the interface between the plywood panels and cold-formed steel joists influenced the natural frequencies of the tested floors. Larger mass and span of composite floor tend to decrease the natural frequencies, whilst higher flexural stiffness increases the natural frequency. For all the tested composite floor

Table 4
Measured natural frequencies (Hz) of the tested composite floors.

	Flexural modes					Torsional modes	
Specimen	*f11*	*f12*	*f13*	*f21*	*f22*	*f1t*	*f2t*
1	19.02	43.906	56.431	88.175	93.87	16.926	40.857
2	21.388	46.906	72.137	91.535	95.247	17.768	44.617
3	21.903	44.183	–	92.014	95.108	17.365	35.903
4	17.53	39.434	64.964	83.238	91.068	14.096	32.098
5	18.968	43.2	69.977	88.42	94.03	15.662	35.139
6	19.588	45.085	68.91	90.023	95.383	17.834	39.1
7	20.624	45.003	65.54	89.15	94.782	17.766	37.947
8	18.18	38.012	57.941	81.84	89.724	16.36	34.94
9	19.592	44.762	59.88	87.412	91.018	17.004	35.17
10	19.156	42.56	56.115	84.239	91.513	16.02	35.857
11	17.8	41.867	66.051	87.433	94.631	15.867	32.86
12	18.936	40.95	62.786	86.78	94.17	16.78	35.08

specimens, the span and mass were maintained constant; however, the flexural stiffness was varied. The fundamental natural frequency of specimen 1 (reference specimen) was 19.020 Hz, whereas f_{11} for specimen 2 was 21.388 Hz. Doubling the number of self-drilling screws in specimen 2 improved the f_{11} by 12.45% compared specimen 1. The enhancement in the fundamental natural frequency is attributed to the high friction force at the interface between plywood and the joist which resulted in a stiffer connection and minimal slip at the interface. Similar behaviour was observed in specimens 3 and 4 (f_{11} = 21.903 Hz and 17.530 Hz, respectively) and specimens 7 and 8 (f_{11} = 20.624 Hz and 18.180 Hz, respectively). The addition of the structural epoxy resin at the interface improved the fundamental natural frequency of specimen 3 by 25% compared to f_{11} of specimen 4, whilst the improvement in specimen 7 was 13.45% compared to f_{11} of specimen 8. Again, higher friction force produced stiffer connection and negligible slip at the interface.

Specimen 5 had twice the number of fasteners than specimen 1 and larger connector diameter; however, specimen 5 had a fundamental natural frequency of 18.968 Hz that is slightly less than the fundamental natural frequency of the reference specimen which had f_{11} = 19.020 Hz. Similarly, insignificant increase (3%) in f_{11} was observed in specimen 6 despite having fasteners diameter twice larger that the SDS connector used in specimen 1. Likewise, a minor decrease (2.30%) was observed in the fundamental natural frequency of specimen 10 (f_{11} = 19.156 Hz) compared to specimen 9 (f_{11} = 19.592 Hz). In general, increasing the number fasteners or using larger diameter connectors or both had insignificant effect on the vibration behaviour of the tested composite floors. Similar observations were reported by Chiniforush et al., [1]. Rijal [4] reported that increasing the number of notches in timber-concrete composite floors had negligible effect on the natural frequencies of the tested floors. Dackermann et al., [41] highlighted that decreasing the number of fasteners by 50% in a composite floor system had no effect on the natural frequencies of the floors.

Vibration discomfort is a serviceability limit state and service loads produce insignificant relative slip at the interface between the plywood panels and cold-formed steel joists. As a result, the friction at the interface governs the connection behaviour between the two materials. Such behaviour is evident from the improved fundamental natural frequency of specimens 3 and 7 which utilise structural epoxy resin used to enhance the friction force at the interface. The higher fundamental natural frequency of specimen 2 was a result of larger normal force applied at the interface which improved the friction force between the plywood panels and cold-formed steel joists. Higher normal force at the interface was achieved by the mechanically driven SDS connectors.

The effect of the utility holes drilled through the joist web was insignificant as evident from the reported values of f_{11} in specimens 11 and 12. Specimens 11 and 8 are identical in terms of geometry and the fastener type and spacing; however, specimen 11 had a fundamental natural frequency of 18.380 Hz which is 1.10% higher than the fundamental natural frequency of the specimen 8 (f_{11} = 18.180 Hz). Similar observations were withdrawn for the identical specimens 12 and 5 (f_{11} = 19.050 Hz for specimen 12 and 18.968 Hz for specimen 5). Cutting utility holes within the webs of the joists slightly reduced the total mass of the composite floors and increased the fundamental natural frequency of the floors as expected.

The measured natural frequencies of the second bending mode (f_{12}) ranged between 38.012 Hz and 46.906 Hz. For all specimens, the average ratio between the second and the first flexural modes natural frequencies was 2.21; though, Rao [42] reported that the analytical ratio should be around 4 for perfectly simply supported beam. The lower ratio between the second and the first flexural modes indicate that the adopted boundary conditions in the tests provided rotational fixity for the supported composite floors. Overall, the first torsional mode (f_{1t}) had the least natural frequency (ranged between 14.096 Hz and 17.834 Hz) in all specimens indicating that the cold-formed steel and plywood composite floors had a lower torsional stiffness compared to the flexural stiffness. However, in real composite floor systems comprised of cold-formed steel joists and plywood panels, the torsional modes will not dominate the vibration behaviour of the floors due to the continuity of the floor panels.

Fig. 13 presents the theoretical fundamental natural frequencies for both full composite and non-composite floors. The fundamental natural frequencies for these floors were calculated using Eq. (3), which assumes an Euler-Bernoulli beam;

$$f_{11} = \frac{\pi}{2L^2}\sqrt{\frac{EI}{\rho_t A_t + \rho_s A_j}} \tag{3}$$

where L is the span of the composite floor, ρ_t and ρ_s are the densities of plywood and cold-formed steel joists, respectively, and A_t and A_j are the cross-sectional areas of the plywood and cold-formed steel joists, respectively. EI is flexural stiffness of the floors and can be determined according to Eqs. (4) and (5);

$$EI_0 = E_t I_t + E_j I_j \tag{4}$$

$$EI_{100} = E_t I_t + E_j I_j + \frac{E_t A_t \bullet E_j A_j}{E_t A_t + E_j A_j} \times \left(\frac{h_t + h_s}{2}\right)^2 \tag{5}$$

In Eqs. (4) and (5), EI_0 and EI_{100} are the non-composite and full composite bending stiffness, respectively, E_t and E_j are the Young's moduli of the plywood and cold-formed steel joists, respectively, I_t and I_j are the second moment of area of the plywood and cold-formed steel joists, respectively, A_t and A_j are the cross sectional area of the plywood and joist, respectively, h_t is the thickness of the plywood panel, and h_s is the depth of the cold-formed steel section. In Eq. (4), the bending stiffness is the summation of the individual stiffness of the plywood and joists since the connection between the two materials does not exist. Accordingly, Eq. (5) essentially combines the individual stiffness

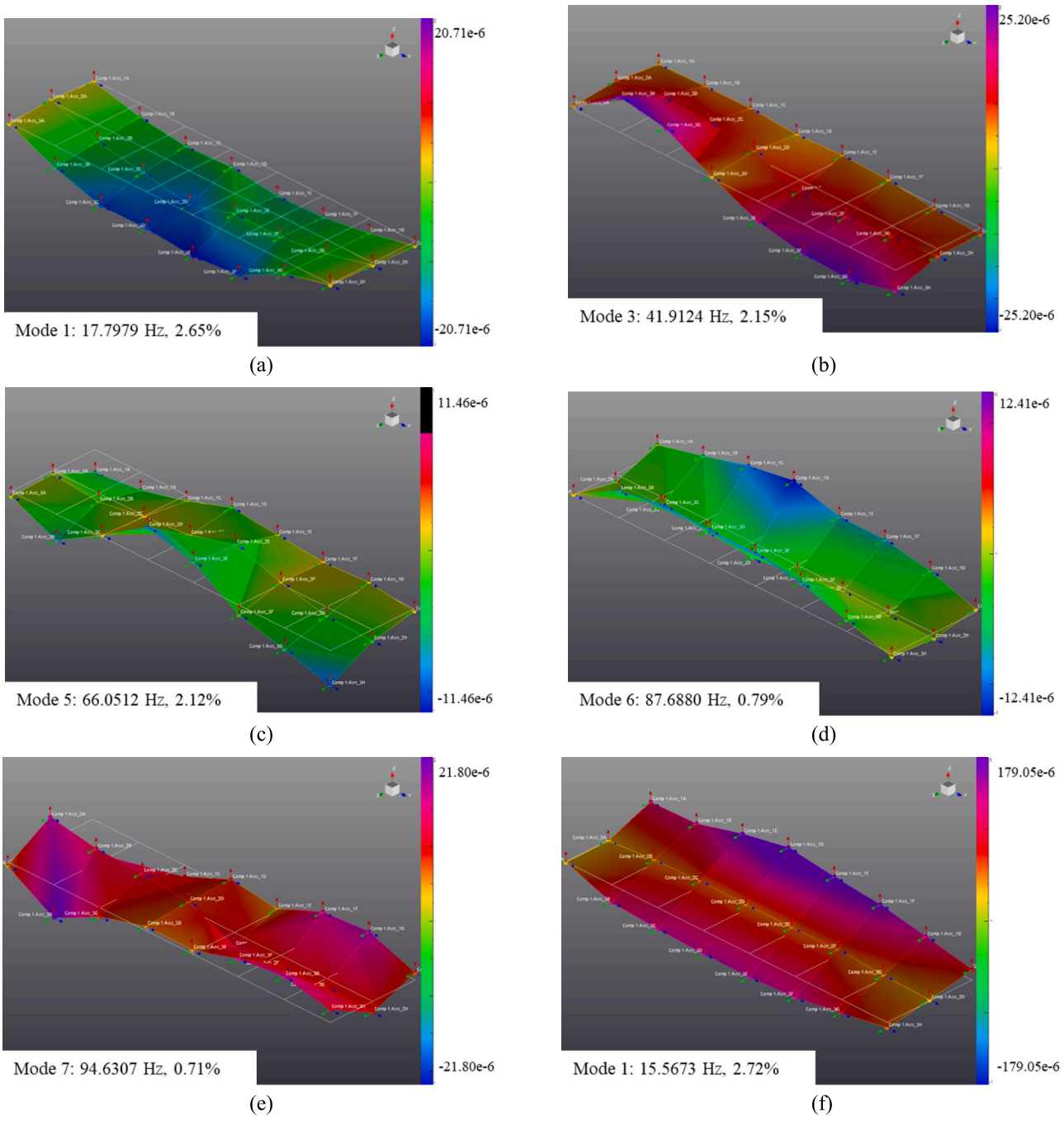

Fig. 8. Typical measured mode shapes of cold-formed steel and plywood composite floors: (a) f_{11}, (b) f_{12}, (c) f_{13}, (d) f_{21}, (e) f_{22}, (f) f_{1t}, and (g) f_{2t}.

contributions of the timber and steel components, considering their respective elastic moduli, moments of inertia, and cross-sectional areas. The last term in the equation represents the geometric adjustment factor based on the centroid location of the materials in relation to the global centroid of the composite section.

It is evident from Fig. 13 that the measured natural frequencies of the cold-formed steel and plywood composite floors are near to that of the full composite floors. Specimens 2, 3, and 7 had the closest natural frequencies to the theoretical value of the full composite floors, because of a relatively high friction force that exists between cold-formed steel and plywood panels due to the influence of glue and post-tensioning force. Thus, the composite joints act as a perfect composite section with minimal slip and higher stiffness. Generally, specimens utilising M8 bolts, M12 bolts, and M12 CS had lower natural frequencies in comparison with specimens using 6 mm SDS fasteners or specimens with structural epoxy applied at the interface of the two materials. The reason for such behaviour is attributed to the looseness provided by the pre-drilled holes in the plywood and joists which significantly affected the degree of friction between the connectors, the plywood panels, and the cold-formed steel joists.

3.3.2. *Damping*

Damping denotes the ability of a system to dissipate energy [43]. In practice, when a system vibrates, its total energy progressively diminishes until it reaches zero, at which point the system stops vibrating. Friction is the primary source of damping in structures. Relative motion

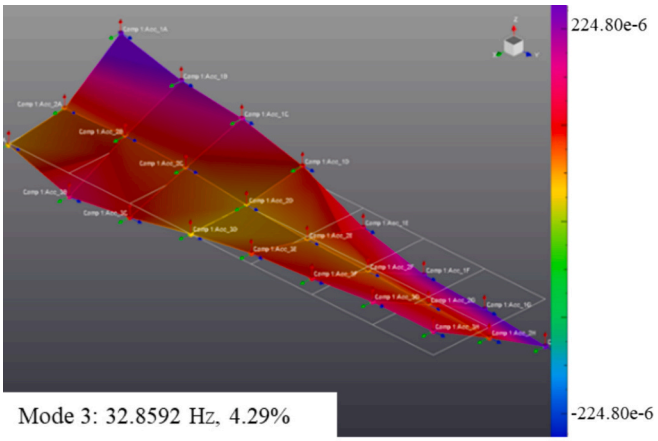

(g)

Fig. 8. (*continued*).

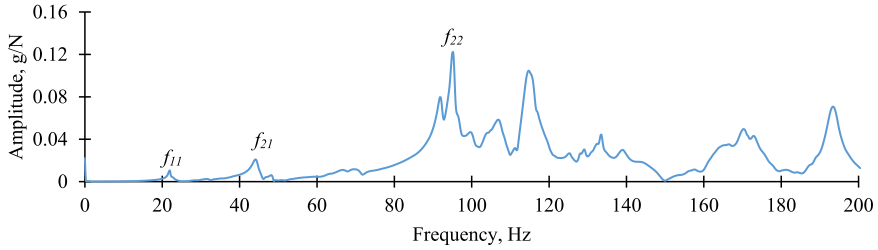

(a) FRF of specimen 3 due to excitation at H1 hammer location.

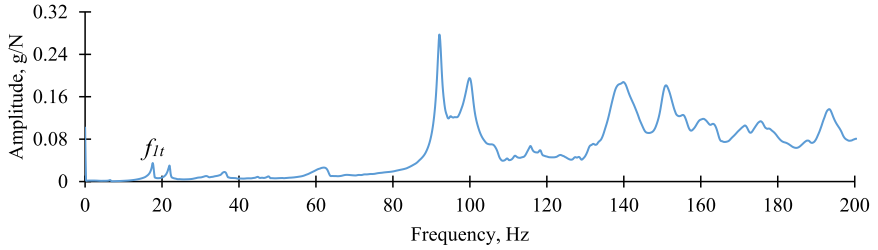

(b) FRF of specimen 3 due to excitation at H3 hammer location.

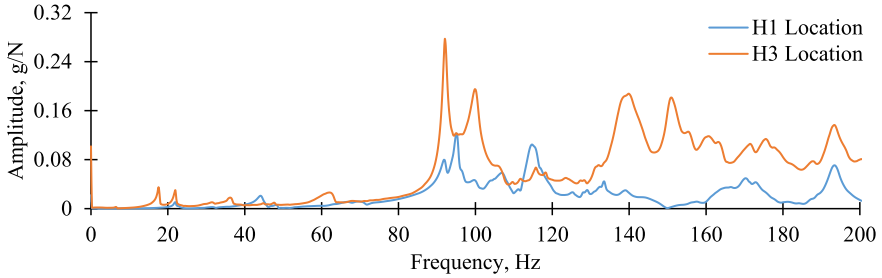

(c) Floor responses comparison when excited at H1 and H3 hammer locations.

Fig. 9. Typical FRFs diagrams of specimen 3 measured at A10 accelerometer location when excited at (a) H1 hammer location, (b) H3 hammer location (c) Comparison of floor responses between hammer locations H1 and H3.

between components of solids in a structure produces internal friction, which contributes to the damping. This type of damping is called structural or hysteretic damping. A different kind of damping generates from the sliding contact between two surfaces, such as bolts and nuts or furniture sliding over a floor; this type of damping is referred to as dry-friction damping. The damping ratios of the first bending mode of the tested composite floors are given in Table 5. Curve fitting of FRF using fraction polynomial method was used to calculate the damping in the tested floors.

As a dimensionless property, damping ratio primarily depends on the actual material damping and stiffness and mass of the floors. As all tested composite floors were identical in terms of materials and mass, the flexural stiffness determined their damping ratios. Regardless of the fastener type, specimens utilising 200 mm spaced connectors had higher

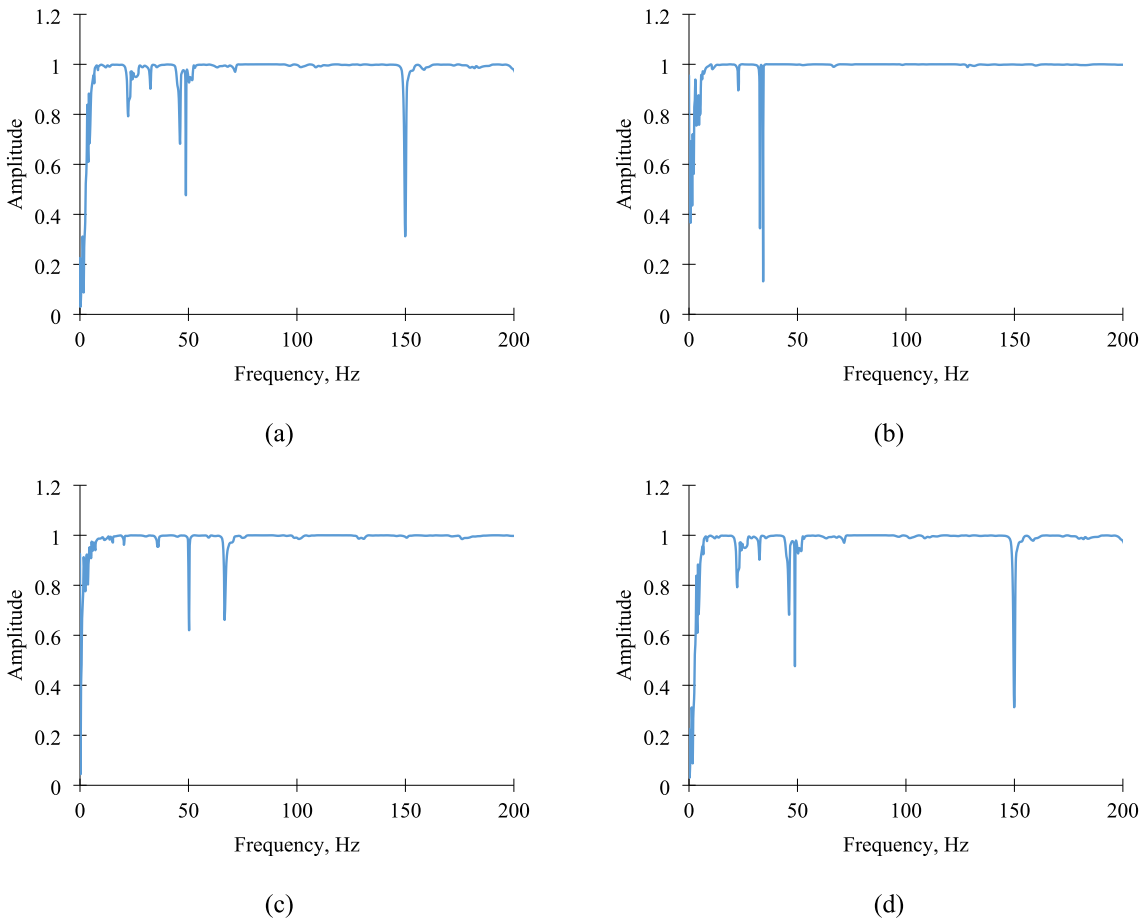

Fig. 10. Coherence functions calculated for FRFs measured at A10 accelerometer due to excitation at H1 hammer location: (a) specimen 2, (b) specimen 3, (c) specimen 6, and (d) specimen 9.

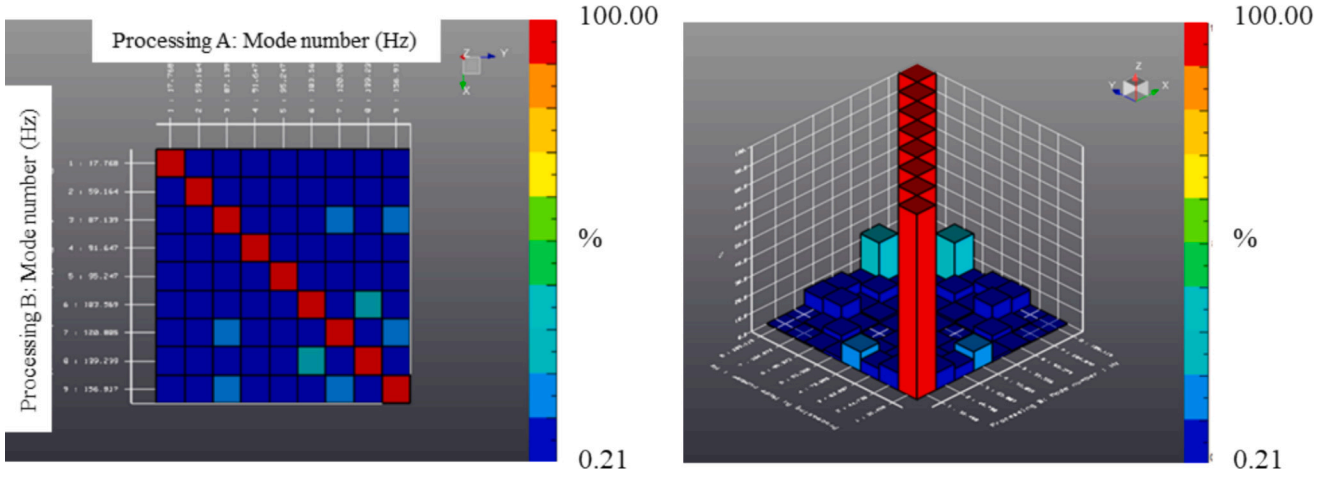

Fig. 11. Modal assurance criterion depicted for specimen 2 (dark blue colour indicates close to zero similarity). (For interpretation of the references to colour in this figure legend, the reader is referred to the web version of this article.)

damping ratios compared to samples with 400 mm and 800 mm connector spacing as depicted in Fig. 14. It was also observed that specimens 3 and 7, which used structural epoxy resin at the interface between the plywood and cold-formed steel joists, had lower damping ratios in comparison with their identical counterparts (specimens 4 and 8, respectively).

Smith et al., [44] and Eurocode 5 [45] suggest a 1.1% and 1%, respectively, typical damping ratio for completely bare floors or floors with minimum furnishings. Except for specimen 6, all tested composite floors had damping ratios higher than 1.1%. Generally, factors that determine damping differ significantly between different structures, thus, it is quite challenging to estimate damping at the design stage. In actual composite floor systems, damping depends on the existence of non-structural elements, for instance partitions, ceilings, and furniture. Hence, larger damping ratios are anticipated in an actual composite floor sitting compared to the damping values reported in this study.

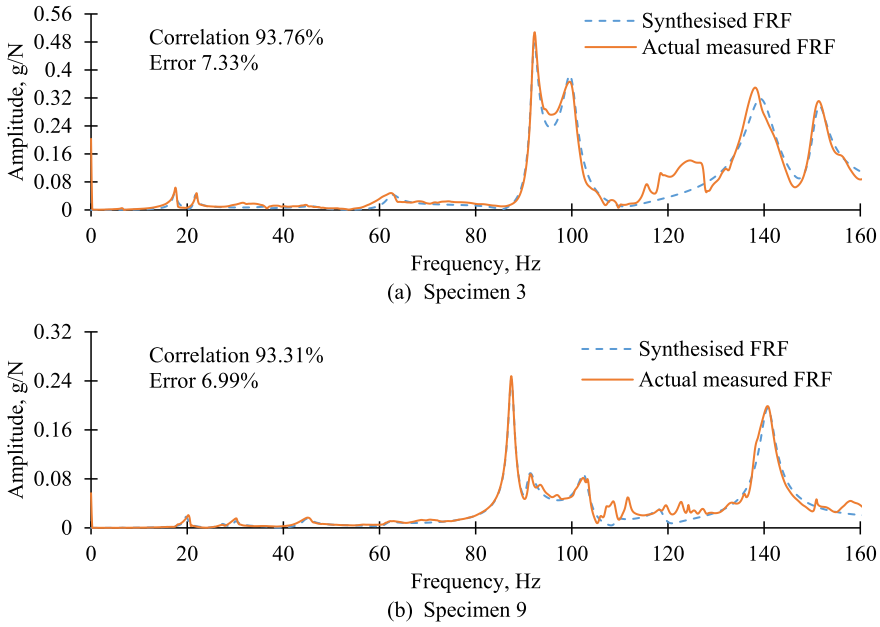

Fig. 12. Comparison of synthesized FRFs and actual measured FRFs calculated for A3 accelerometer for specimens 3 and 9.

Table 5
Synthesized FRFs correlations and their corresponding error values compared to the actual measured FRFs.

Specimen	1	2	3	4	5	6	7	8	9	10	11	12
Correlation	95.47	94.28	92.67	93.72	93.14	94.76	93.41	93.84	93.01	94.66	94.02	93.78
Error	4.53	5.72	7.33	6.28	6.86	5.24	6.59	6.16	6.99	5.34	5.98	6.22

Table 6
Damping ratios of the tested plywood and cold formed steel composite floors.

Specimen	Fastener	Spacing	Glue	Holes	Damping, (%)
1	SDS 6 mm	400			2.97
2		200			3.39
3		400	TRUE	FALSE	2.13
4	M12 CS	400			2.66
5		200			2.64
6		400			0.86
7	M12 Bolts	800	TRUE	FALSE	1.16
8		800			1.91
9	M8 Bolts	200			2.22
10		400			1.81
11	M12 Bolts	800	FALSE	TRUE	2.65
12	M12 CS	200	FALSE	TRUE	1.89

3.3.3. *Flexural stiffness*

Once the cross-section geometry (mass) and span of the composite floors were determined and maintained constant, the flexural stiffness became the governing factor to decide the serviceability performance for the composite floors subjected to static and dynamic loads. Previous research on cold-formed steel and plywood composite floors extensively investigated the static of such composite floors; however, the static properties obtained from the static tests may not be applicable to determine the dynamic performance of the cold-formed steel and plywood composite floors. In this section, the dynamic flexural stiffness determined from vibration tests is compared to static flexural stiffness measured from the 1 kN point load deflection testes and four-point bending tests. It is noted that the authors have made a deliberate choice to exclusively employ the Bernoulli beam equation for comparison with vibration due to its relevance and suitability for the specific context of their study. While alternative methods such as the Murray method [29] or CLT design guide methodology [46] developed by

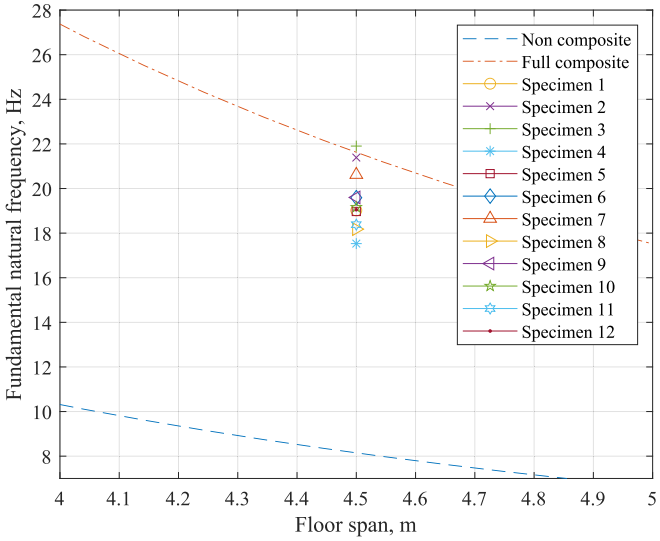

Fig. 13. Theoretical fundamental natural frequencies (full composite and non-composite) compared to measured fundamental natural frequencies of the tested floors.

Woodworks exist, the decision to focus on the Bernoulli beam equation may have been influenced by factors such as its widespread acceptance and specific objectives and scope of the research, limitations in resources, and a deliberate focus on a particular analytical approach for consistency and comparability within the study.

According to the Euler – Bernoulli beam theory, the dynamic flexural stiffness, EI_d, (referred to as dynamic stiffness) was calculated from the fundamental natural frequency of the tested specimens by neglecting

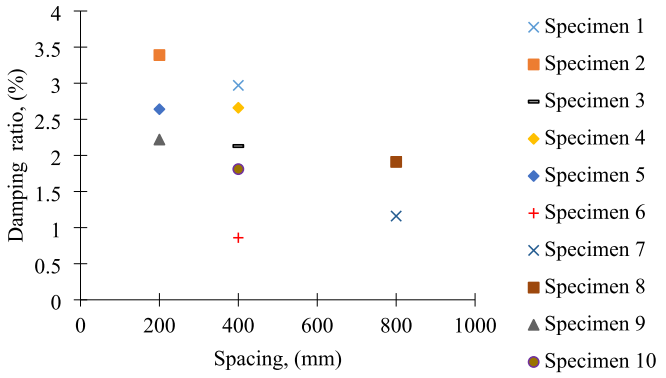

Fig. 14. Comparison of measured damping ratios of the first bending mode against spacing of fasteners for specimens 1 through 10.

shear deformations in the floors. According to Eq. (6), the dynamic stiffness is estimated as

$$EI_d = (\rho_t A_t + \rho_s A_s)\left(\frac{2L^2 f_{11}}{\pi}\right)^2 \quad (6)$$

The notations in Eq. (6) are the same as in Eq. (3). Accordingly, the static flexural stiffness predicted from 1 kN point load deflection tests, EI_s, (referred to as static stiffness) is calculated using Eq. (7) [47];

$$EI_s = \frac{L^3}{48} \times \frac{w}{\delta} \quad (7)$$

where L is the span of the tested floor, w is the applied 1 kN point load, and δ is the measured mid-span deflection from the tests.

The static flexural stiffness measured from the four-point bending tests, EI_b, (referred to as bending stiffness) is calculated according to Eq. (8) [47]. The full test results of the four-point flexural tests were discussed in a separate project; however, the pertinent bending stiffness results are discussed here.

$$EI = \frac{a}{48}\left(3L^2 - 4a^2\right)\frac{P}{\delta} \quad (8)$$

where L is the span, a is shear span, and P/δ is the slope of the load-deflection curve between $0.1P_u$ and $0.4P_u$, which is the load level at serviceability limit state according to BS EN 26891 [48]. The flexural stiffness of the tested cold-formed steel and plywood composite floors calculated from the vibration, deflection, and four-point bending tests are listed in Table 7. Moreover, the measured flexural stiffness of the tested floors along with the theoretical flexural stiffness for full composite and non-composite floors are depicted in Fig. 15. As apparent from Fig. 15, the dynamic stiffness of the cold-formed steel and plywood composite floors was higher compared to static stiffness except for specimens 6 and 8. Overall, of the three measured stiffness values, the bending stiffness was the lowest. Unlike static and bending stiffness, the dynamic stiffness was the least influenced by the spacing of fasteners and its type. As expected, specimens utilising 200 mm fasteners spacing had lower mid-span deflection values in comparison with specimens with 400 mm and 800 mm spacing.

The dynamic stiffness of specimens 1 and 2 was 63% and 69% higher than their static stiffness even though specimen 2 had lower mid-span deflection. The reason is that the dynamic stiffness of specimen 2 was 26.50% larger than the dynamic stiffness of specimen 1. The high friction at the interface between the plywood panels and the joists resulted in higher values of the fundamental natural frequency and larger dynamic stiffness accordingly. Specimen 4 had a relatively high mid-span deflection which resulted in a lesser static stiffness compared to the reference specimen (specimen 1). Accordingly, the dynamic stiffness of specimen 4 was 133% larger than its static stiffness. Specimen 5 had similar stiffness values (dynamic and static) in comparison with the reference specimen. Specimens 6 and 8 had their dynamic stiffness less than the static stiffness due to the small measured mid-span deflection. Static stiffness of specimens 6 and 8 was 53% and 20% larger than their dynamic stiffness. Such behaviour indicated that the static stiffness is more sensitive to the variations in the degree of composite action. Dynamic stiffness of specimen 9 was slightly higher compared to the dynamic stiffness of the reference specimen; however, its static stiffness was 37% higher than the static stiffness of the reference specimen. Similarly, specimen 10 had a dynamic stiffness 46% larger than its static stiffness. In conclusion, the static stiffness was more perceptive to the change in the connectors spacing and type, whilst the dynamic stiffness was primarily determined by the degree of friction at the interface between the plywood panels and cold-formed steel joists.

Among the three stiffnesses, the bending stiffness had the lowest value. Such behaviour can be attributed to deformations at the service and ultimate load levels. In modal testing, the deformations of the tested composite floors were insignificant and the slip between the plywood and cold-formed steel joists was negligible. The slip resistance between the two materials was mainly provided by the friction, whilst it was less sensitive to the fasteners type and/or spacing. Likewise, the deformation level in the 1 kN point load static tests was relatively small (in the range of 0.45 mm to 2.01 mm) which indicates that the behaviour of the tested floor was elastic, and that the friction still contributes to the floor flexural stiffness. Conversely, owing to the high deformations, the bending stiffness of the floors was primarily determined by the degree of the composite action provided by bolts or screws. At ultimate loads, cold-formed steel and plywood panels tend to have dissimilar curvatures which implies that the friction contribution to the composite action is negligible.

Table 7
Flexural stiffness of the tested composite floors measured from different tests.

Specimen	Deflection (mm)	f_{11} (Hz)	Dynamic stiffness (kNm^2)	Static stiffness (kNm^2)	Bending stiffness (kNm^2)
1	1.19	19.020	2596	1595	1484
2	0.98	21.388	3282	1937	1689
3	–	21.903	3442	–	–
4	2.01	17.530	2205	944	897
5	1.18	18.968	2581	1609	1436
6	0.45	19.588	2753	4219	1825
7	–	20.624	3052	–	–
8	0.67	18.180	2371	2833	1836
9	0.87	19.592	2754	2182	1925
10	1.05	19.156	2631	1808	1731
11	–	17.800	2273	–	–
12	–	19.050	2604	–	–

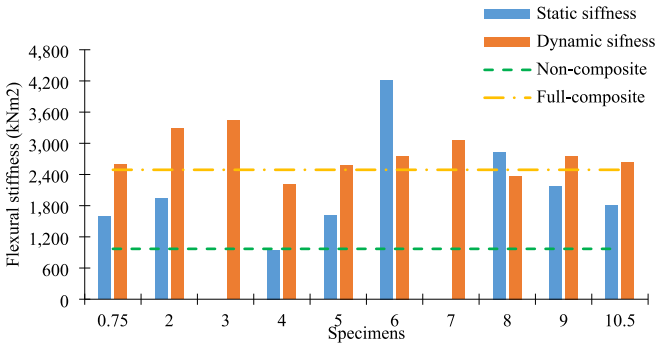

Fig. 15. Flexural stiffness of cold-formed steel and plywood composite floors determined from vibration, deflection, and four-point flexural tests.

4. Conclusion

A comprehensive experimental study was carried out to investigate the vibration behaviour of the cold-formed steel and plywood composite floors. The tested composite floors consisted of two cold-formed steel joists (254 mm deep and 2.40 thick) connected to two plywood panels (1.20 m × 2.40 m × 45 mm) using various types of shear connectors; M6 self-drilling screws, M8 bolts, M12 coach screws, and M12 bolts. Three floor specimens utilising M6 SDS, M12 CS, and M12 bolts coupled with structural epoxy adhesive at the interface between the joists and the plywood panels were also tested. The total length of the composite floors was 4.70 m, whereas the supported span was 4.50 m.

Fundamental natural frequencies obtained from the modal tests proved that the friction at the interface between the joists and plywood panels governed the connection behaviour between the two materials. Such behaviour is evident from the improved fundamental natural frequency of specimens 3 and 7 which utilised structural epoxy resin at the interface between the two materials to enhance the friction force at the interface. The higher fundamental natural frequency of specimen 2 was a result of larger normal force applied at the interface which improved the friction force between the plywood panels and cold-formed steel joists. Higher normal force at the interface was achieved by the mechanically driven SDS connectors.

In contrary, experimental modal tests concluded that increasing the number fasteners (i.e., narrower fastener spacing) or using larger diameter connectors or both had insignificant effect on the natural frequencies of the tested composite floors. Using a wider fastener spacing by factor of 2.0 in specimen 10 slightly reduced the fundamental natural frequency by 2.30% compared to specimen 9 which had double number of shear connectors. However, spacing of fasteners affected the mid-span deflection under the action of 1 kN concentrated load at mid-span. Specimens utilising 200 mm fasteners spacing had lower mid-span deflection values in comparison with specimens with 400 mm and 800 mm spacing. Wider spacing produced higher mid-span deflections, which would result in unsatisfactory vibration behaviour if the deflection limit were exceeded.

Furthermore, the flexural stiffness of the tested cold-formed steel and plywood composite floors was calculated from the vibration, deflection, and four-point bending tests. It was shown that the dynamic stiffness of the cold-formed steel and plywood composite floors was higher compared to static stiffness except for specimens 6 and 8. Overall, of the three measured stiffness values, the bending stiffness was the lowest. Unlike static and bending stiffness, the dynamic stiffness was the slightest influenced by the spacing of fasteners and its type. In conclusion, the static stiffness was more perceptive to the change in the connectors spacing and type, whilst the dynamic stiffness was primarily determined by the degree of friction at the interface between the plywood panels and cold-formed steel joists.

Moreover, Damping, while an integral aspect of this study, was briefly addressed in Section 3.3.2 to underscore the measured damping values and to compare them with the recommended values stipulated in applicable standards. An in-depth examination of damping in structural floor systems could indeed serve as a promising avenue for future research endeavours.

Lastly, it is important to note that a comprehensive analysis addressing an appropriate design limit, which considers both the mid-span deflection and the fundamental natural frequency, has been previously discussed in our prior publication [33]. We highly recommend reviewing this publication alongside the current study for a more comprehensive understanding of the design considerations and recommendations. This prior work provides valuable insights that complement and contextualise the findings presented in the present study, thereby enriching the overall understanding of the subject matter.

CRediT authorship contribution statement

Suleiman A. Al-Hunaity: Writing – original draft, Visualization, Validation, Software, Methodology, Investigation, Formal analysis, Data curation, Conceptualization. **Harry Far:** Writing – review & editing, Validation, Supervision, Methodology, Investigation, Conceptualization.

Declaration of competing interest

The authors declare that they have no known competing financial interests or personal relationships that could have appeared to influence the work reported in this paper.

Data availability

Data will be made available on request.

References

[1] A. Chiniforush, M. Makki Alamdari, U. Dackermann, H.R. Valipour, A. Akbarnezhad, Vibration behaviour of steel-timber composite floors, Part (1): experimental & numerical investigation, J. Constr. Steel Res. 161 (2019) 244–257.
[2] A. Ebrahimpour, R.L. Sack, Design live loads for coherent crowd harmonic movements, J. Struct. Eng. 118 (1992) 1121–1136.
[3] S.A. Al Hunaity, H. Far, A. Saleh, Vibration behaviour of cold-formed steel and particleboard composite flooring systems, Steel Compos. Struct. 43 (2022) 403–417.
[4] R. Rijal, Dynamic Performance of Timber and Timber-Concrete Composite Flooring Systems, University of Technology Sydney, NSW, Australia, 2013.
[5] L. Xu, S. Zhang, C. Yu, Determination of equivalent rigidities of cold-formed steel floor systems for vibration analysis, part II: evaluation of the fundamental frequency, Thin-Walled Struct. 132 (2018) 1–15.
[6] L. Xu, Floor vibration performance of lightweight cold-formed steel framing, Adv. Struct. Eng. 14 (2011) 659–672.
[7] C. Loss, M. Piazza, R. Zandonini, Connections for steel–timber hybrid prefabricated buildings. Part II: innovative modular structures, Constr. Build. Mater. 122 (2016) 796–808.
[8] H. Far, A. Saleh, A. Firouzianhaji, A simplified method to determine shear stiffness of thin walled cold formed steel storage rack frames, J. Constr. Steel Res. 138 (2017) 799–805.
[9] A. Saleh, H. Far, L. Mok, Effects of different support conditions on experimental bending strength of thin walled cold formed steel storage upright frames, J. Constr. Steel Res. 150 (2018) 1–6.
[10] X. Li, M. Ashraf, M. Subhani, P. Kremer, H. Li, M. Anwar-Us-Saadat, Rolling shear properties of cross-laminated timber (CLT) made from Australian Radiata pine – an experimental study, Structures 33 (2021) 423–432.
[11] A. Dodoo, L. Gustavsson, R. Sathre, Lifecycle carbon implications of conventional and low-energy multi-storey timber building systems, Energ. Build. 82 (2014) 194–210.
[12] S. Navaratnam, D. Widdowfield Small, P. Gatheeshgar, K. Poologanathan, J. Thamboo, C. Higgins, et al., Development of cross laminated timber-cold-formed steel composite beam for floor system to sustainable modular building construction, Structures 32 (2021) 681–690.
[13] K. Thirunavukkarasu, E. Kanthasamy, P. Gatheeshgar, K. Poologanathan, H. Rajanayagam, T. Suntharalingam, et al., Sustainable performance of a modular building system made of built-up cold-formed steel beams, Buildings 11 (2021) 460.
[14] C. Wang, T.-M. Chan, Seismic design and parametric study of steel modular frames with distributed seismic resistance, Thin-Walled Struct. 182 (2023) 110325.
[15] S.A. Al-Hunaity, D. Karki, H. Far, Shear connection performance of cold-formed steel and plywood composite flooring systems: experimental and numerical investigation, Structures 48 (2023) 901–917.
[16] N. Vella, L. Gardner, S. Buhagiar, Experimental analysis of cold-formed steel-to-timber connections with inclined screws, Structures 24 (2020) 890–904.
[17] P. Kyvelou, L. Gardner, D.A. Nethercot, Finite element modelling of composite cold-formed steel flooring systems, Eng. Struct. 158 (2018) 28–42.
[18] R. Yang, H. Li, R. Lorenzo, M. Ashraf, Y. Sun, Q. Yuan, Mechanical behaviour of steel timber composite shear connections, Constr. Build. Mater. 258 (2020) 119605–119623.
[19] M. Abu-Hamd, Experimental study on screw connections in cold-formed steel walls with cement sheathing, Adv. Struct. Eng. 22 (2019) 2033–2047.
[20] A. Hassanieh, H.R. Valipour, M.A. Bradford, Experimental and numerical study of steel-timber composite (STC) beams, J. Constr. Steel Res. 122 (2016) 367–378.
[21] L. Zhang, Y.H. Chui, D. Tomlinson, Experimental investigation on the shear properties of notched connections in mass timber panel-concrete composite floors, Constr. Build. Mater. 234 (2020) 117375.
[22] A. Hassanieh, H.R. Valipour, M.A. Bradford, Load-slip behaviour of steel-cross laminated timber (CLT) composite connections, J. Constr. Steel Res. 122 (2016) 110–121.

[23] J. Negreira, Vibrations in Lightweight Buildings Perception and Prediction, Lund University, Sweden, 2013.
[24] J. Negreira, A. Trollé, K. Jarnerö, L.G. Sjökvist, D. Bard, Psycho-vibratory evaluation of timber floors - towards the determination of design indicators of vibration acceptability and vibration annoyance, J. Sound Vib. 340 (2015) 383–408.
[25] L. Zhang, J. Zhou, Y.H. Chui, G. Li, Vibration performance and stiffness properties of mass timber panel–concrete composite floors with notched connections, J. Struct. Eng. 148 (2022) 04022136.
[26] X. Zhou, Y. Shi, L. Xu, X. Yao, W. Wang, A simplified method to evaluate the flexural capacity of lightweight cold-formed steel floor system with oriented strand board subfloor, Thin-Walled Struct. 134 (2018) 40–51.
[27] H. Du, X. Hu, Z. Sun, Y. Meng, G. Han, Load carrying capacity of inclined crossing screws in glulam-concrete composite beam with an interlayer, Compos. Struct. 245 (2020) 112333.
[28] D. Karki, H. Far, A. Saleh, Numerical studies into factors affecting structural behaviour of composite cold-formed steel and timber flooring systems, J. Build. Eng. 44 (2021) 102692.
[29] T.M. Murray, D.E. Allen, E.E. Ungar, D.B. Davis, AISC Design Guide 11. Vibrations of Steel-Framed Structural Systems Due to Human Activity, United States of America: American Institute of Steel Construction, 2016.
[30] L. Cao, Y. Tan, J. Li, Experimental studies on vibration serviceability of composite steel-bar truss slab with steel girder under human activities, Steel Compos. Struct. 40 (2021) 663–678.
[31] D. Casagrande, I. Giongo, F. Pederzolli, A. Franciosi, M. Piazza, Analytical, numerical and experimental assessment of vibration performance in timber floors, Eng. Struct. 168 (2018) 748–758.
[32] International Organization for Standardization, ISO 10137. Bases for Design of Structures-Serviceability of Buildings and Walkways against Vibrations. Geneva, Switzerland, 2007.
[33] S.A. Al-Hunaity, H. Far, Vibration performance evaluation of cold-formed steel and plywood composite floors, Int. J. Struct. Stab. Dyn. 2450269 (2024).
[34] D. Karki, S. Al-Hunaity, H. Far, A. Saleh, Composite Connections between CFS Beams and Plywood Panels for Flooring Systems: Testing and Analysis, Structures: Elsevier, 2022, pp. 771–785.
[35] Standards Australia, AS 1110.2. ISO Metric Hexagon Bolts and Screws - Product Grades A and B - Screws, Australia, SAI Global, 2015.
[36] Standards Australia, AS 1112.1. ISO Metric Hexagon Nuts - Style 1 - Product Grades A and B, SAI Global, Australia, 2015.
[37] Á. Cunha, E. Caetano, Experimental modal analysis of civil engineering structures, Sound Vibrat. 40 (2006) 12–20.
[38] D.J. Ewins, Modal Testing: Theory, Practice and Application Baldock, Hertfordshire, England, Research Studies Press, Philadelphia, PA, 2000.
[39] Siemens Digital Industries Software, Simcenter Testlab 2206, Siemens, 2021.
[40] P. Avitabile, Modal Testing: A Practitioner's Guide, John Wiley & Sons, 2017.
[41] U. Dackermann, J. Li, R. Rijal, K. Crews, A dynamic-based method for the assessment of connection systems of timber composite structures, Constr. Build. Mater. 102 (2016) 999–1008.
[42] S.S. Rao, Vibration of Continuous Systems, John Wiley & Sons Inc., Hoboken, New Jersey, United States, 2007.
[43] A.A. Shabana, Theory of Vibration: An Introduction, Springer, New York, United States, 2012.
[44] A.L. Smith, S.J. Hicks, P.J. Devine, Design of Floors for Vibration: A New Approach, Steel Construction Institute Ascot, Berkshire, UK, 2009.
[45] European Committee for Standardization, Eurocode 5. Eurocode 5: Design of Timber Structures-Part 1–1: General-Common Rules and Rules for Buildings, European Committee for Standardization, Brussels, Belgium, 2004.
[46] Wood Products Council, Mass Timber Design Manual – Volume 2, 2023.
[47] ASTM, Standard Test Methods of Static Tests of Lumber in Structural Sizes. ASTM D198–15, ASTM, West Conshohocken, 2015.
[48] BS EN 26891, Timber Structures - Joints Made with Mechanical Fasteners - General Principles For The Determination of Strength and Deformation Characteristics, British Standards, 1991.